Research and Reviews in Materials Science and Chemistry
Vol. 7, Issue 1, 2016, Pages 25-42
ISSN 2319-6920
Published Online on October 8, 2016

http://jyotiacademicpress.org

A REMARKABLE IMPROVEMENT OF IONIC CONDUCTION IN AN ENVIRONMENTAL FRIENDLY GLASSY LITHIUM ELECTROLYTE

P. E. DI PRÁTULA, S. TERNY, M. E. SOLA and M. A. FRECHERO

Departamento de Química
Universidad Nacional del Sur (UNS)
Av. Alem 1253
CP 8000-Bahía Blanca
Argentina
e-mail: frechero@uns.edu.ar

Abstract

A new modified lithium-phosphate glass has been obtained by environmentally friendly components. This glass has provided a remarkable lithium ion solid electrolyte. Frequency-dependent electrical data of several lithium-phosphate glass compositions has been discussed in the framework of the electric modulus representation. The origin of the non-Debye behaviour of relaxations (distribution of relaxation times) has been discussed in terms of inter-ionic Coulombic interactions. Structural properties studied by X-ray diffraction, density and FTIR are correlated to the electrical behaviour of the glass. The material electrical behaviour suggests an exceptional candidate for being solid electrolyte in all solid state lithium ion batteries.

Keywords and phrases: lithium, solid state battery, low environmental impacts, novel lithium bismuthate glass, ionic conductivity.

Communicated by Ana Rosa Silva.

Received March 28, 2016; Revised September 8, 2016

1. Introduction

During the last 25 years, lithium batteries have become the favorite energy accumulators. Such choice is supported by its high energy density, light weight design and long lifespan [1]. Moreover, society expects to eliminate its dependence on fossil fuels [2]. Neither more nor less. However, many questions have emerged. Are lithium reserves enough to cover for this huge need? Is the enormous variety of designed materials *the best* for batteries as it has been proclaimed? [3] Are batteries safe enough? [4] Is its development and massive use really sustainable, both in terms of money and the environment? [5]

In the present work, we report a lithium glassy ionic conductor which considers the aforementioned points. We use environmentally friendly components which are low cost and which can be eventually recycled. Perhaps, a new look at the simplest and most well-known materials is the answer to our search.

Phosphate glasses have been studied for several decades because of their behaviour as electronic, ionic or mixed conductors, depending on the components they are mixed with. On the other hand, pure bismuthate glasses are difficult to obtain. In the literature, there are several works refer to bismuthate as an unconventional glass former [6, 7]. However, phosphate and bismuthate together result in a glass which has many intriguing properties. Bismuth ions are highly polarizable and can exist in the glass network in $[BiO_3]$ pyramidal units in the presence of conventional glass-forming ions such as (P^{5+}) [8, 9]. The introduction of alkali ions in bismuthate glasses exhibit high electrical conductivity, hence they can be applied as solid electrolytes in high energy density batteries and sensors [10]. Additionally, phosphate is abundant in the Earth's crust and in ecological terms it is important for biological systems because it is a nutrient in environments. Make a glass material by a standard melt quenching technique is the ancient method, easy and widely known, and it does not required sophisticated technical

equipment. Incorporation of extra oxides permits to obtain a more chemical stable glassy matrix, with an extraordinary capacity to contain large amount of very mobile lithium ions.

In this work, we report some modifications in phosphate-bismuthate glass which allow huge improvements in their electrical properties because of the changes in the 3D structure making them exceptional candidates for being solid electrolytes in solid lithium ion batteries. Frequency-dependent electrical data of several lithium-phosphate glass compositions has been discussed in the framework of the electric modulus representation. The origin of the non-Debye behaviour of relaxations (distribution of relaxation times) has been discussed in terms of inter-ionic Coulombic interactions [11].

2. Experimental

Samples of this work were prepared by a standard melt quenching technique using reagent grade chemicals of $BaCO_3$, Li_2CO_3, Bi_2O_3, and $H_2(NH_4)PO_4$. From now: **LBPB** = $19BaO\ (74P_2O_5\ 7Bi_2O_3)$; **LBPB1** = $19Li_2O\ 16BaO\ (58P_2O_5\ 7Bi_2O_3)$; **LBPB2** = $24Li_2O\ 15BaO\ (55\ P_2O_5\ 6Bi_2O_3)$; **LBPB3** = $32Li_2O\ 32BaO\ (32P_2O_5\ 4Bi_2O_3)$; **LBPB4** = $42\ Li_2O\ 18BaO\ (36P_2O_5\ 4Bi_2O_3)$; **LBPB5** = $55Li_2O\ 8BaO\ (33P_2O_5\ 4Bi_2O_3)$; every composition is expressed in mol% and between parenthesis are the oxides that form the glassy matrix.

Every composition was prepared weighting the appropriate amounts of the components (according to each formula expressed above). The powders were well mixed in an agate mortar and next were placed in a platinum crucible in order to obtain 5g of glass by batch. The decarboxylation and ammonia elimination process was done at a lower temperature than the mix melting point and, when the effervescence finished, the mix was heated for one hour in an electric furnace until it reached a temperature of 1323K. During the process, the crucible was shaken frequently to ensure homogenization and to avoid the retention of

gases in the melt. Next, the molten material was poured in the form of drops on a preheated aluminum plate and held for annealing at 250ºC during 2h, in order to relax the mechanical stress retained at the quenching.

Amorphous character of the samples was tested by X-ray diffraction (XRD) analysis. The XRD patterns of powdered samples, after the annealing, was performed with PW1710 BASED in continuous scan mode with a copper anode and 45KV- 30mA for the tension and electrical current generator respectively. Samples were exposed to the CuK_{α} radiation ($\lambda = 1.54\text{Å}$) at room temperature in the 2θ range: 3º-60º. X-ray fluorescence analysis (XRF) was carried out in a PANalytical Magi'X in He atmosphere. Glass transition temperature (T_g) of each sample was registered by DTA heating it at 10K.min^{-1}, starting from room temperature up to 1000ºC, using 20mg of glass previously crashed in an agate mortar.

Every sample was polished with very fine sand paper in order to obtain glass disks with two parallel faces with thickness ranging between 0.5 and 0.7mm and each face was coated uniformly with a thin layer of silver paint with the purpose of having proper electrical contact. Impedance measurements were carried out with Agilent LCR meter 4284A (20Hz - $1 \cdot 10^6$ Hz; AC voltage amplitude of 0.80V) in a temperature range between room temperature and $(T_g - 15)$ºC.

Room-temperature densities were determined by the Archimedes's principle using 2-propil alcohol as the immersion liquid, being the informed values the average of three independent determinations.

To obtain FTIR spectra, each glass sample was previously ground in an agate mortar to obtain a very fine powder. A semi-quantitative dispersion of each powdered sample in Nujol was registered on a Nicolet Nexus FTIR instrument, in the 2000-400cm^{-1} range, at room temperature, using KBr windows.

3. Results

Figure 1 shows the X-ray diffraction results. There are no sharp peaks in any pattern confirming that each prepared sample is a glass. However, two different deviations on the pattern's base line are clear.

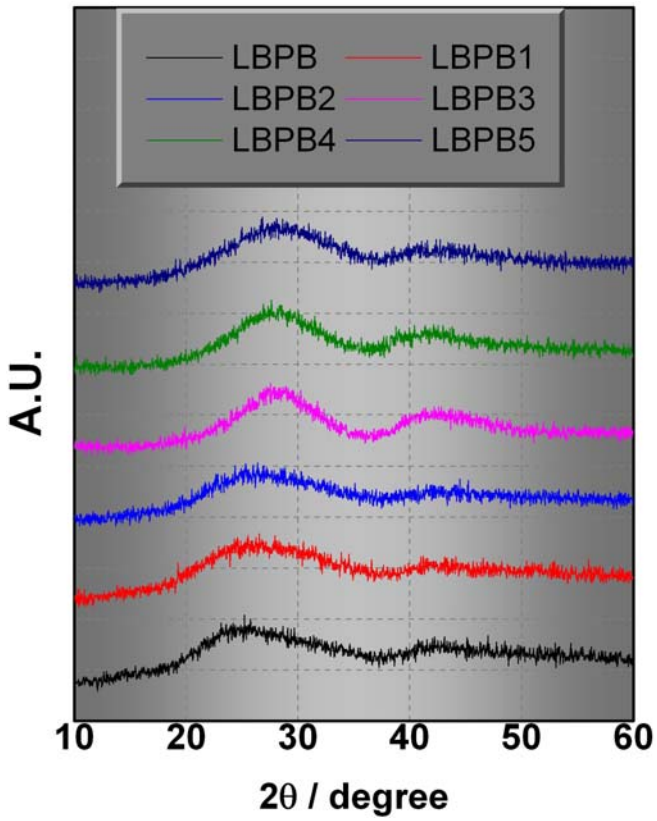

Figure 1. X-ray diffraction patterns of the studied systems.

Figure 2 shows the density values of the studied glasses. The density values of every composition are in the range between 2.9 to 3.8g.cm^{-3}. Considering that the replacement of BaO by P_2O_5 involves similar masses, the first decrease is attributable to the incorporation of Li_2O since the ratio P_2O_5/BaO is similar in both samples (3.9 and 3.6); the following change on the density is influenced not only by the increase of

the content of Li_2O (LBPB2 and LBPB3) but also by the strongly variation on the ratio P_2O_5/BaO from 3.6 to 1.0. It is clear that we need a different perspective to understand the changes induced in this special 3D order in the matrix. Therefore, we have analyzed the magnitude of the oxygen packing density (OPD) [12, 13, 14] that hosts the other atoms who are responsible for the density variation observed. Considering a glass as a three dimensional framework of connected oxygen-phosphorus polyhedra mainly by covalent bonds, the OPD = the number of mol of oxygen atoms per dm^3 of glass, becomes a relevant quantity to analyze the compactness of the skeleton and the variations on it provoked by a modifier oxide.

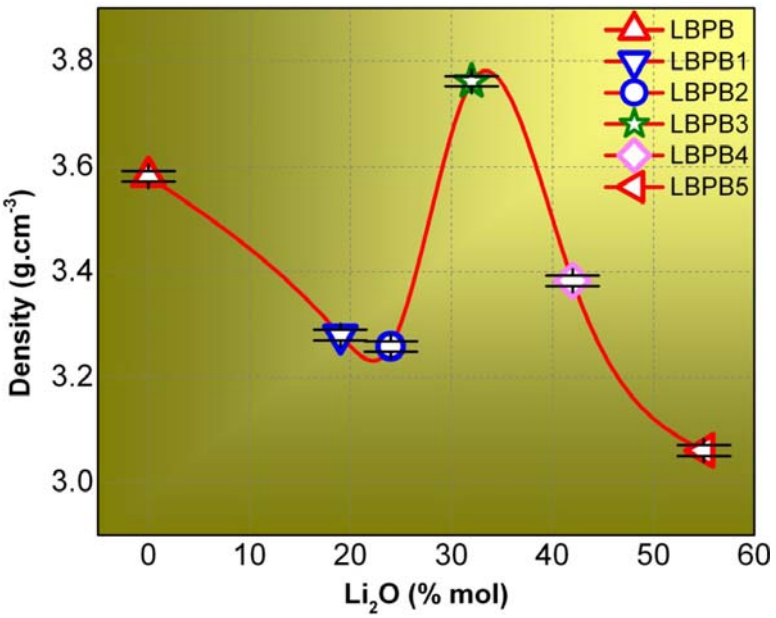

Figure 2. Density values as a function of the Li_2O content.

Figure 3 shows the oxygen packing density (OPD: the number of mol of oxygen per dm^3 of glass), a magnitude that becomes relevant to analyze the compactness of a structure. From these results, it is clear that a stronger modification in the matrix is induced by the incorporation

of lithium oxide rather than the incorporation of barium oxide. Then, the expansion observed in the net of oxygen atoms has a direct relationship with the monovalent cation. After the incorporation of the lithium oxide, the OPD only fluctuate around a similar value (which have been reduced in 14% in respect of the OPD of the no modified glassy matrix). We conclude that the subsequent increases of lithium content finds free space available enough to fit every lithium ion in it without major network expansion.

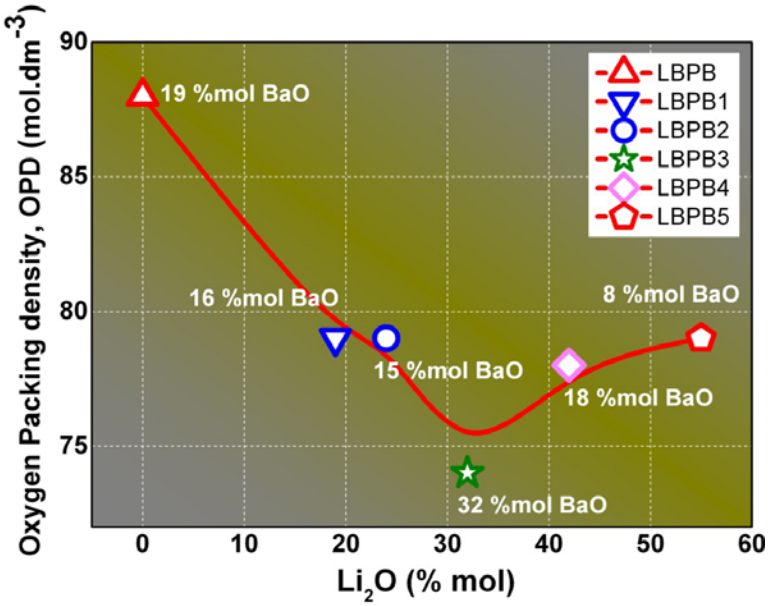

Figure 3. Oxygen packing density (OPD = the number of mol of oxygen per dm^3 of glass) as a function of the Li_2O content.

Figure 4 shows the corresponding T_g as a function of Li_2O content for every studied glass system. From this figure, we learn that T_g value decreases as the lithium content increases. This monotonous behaviour with the increase of modifier content is frequently observed in the mostly of the oxide glasses. It is worth noting, that the effect of increasing the T_g value is due to the incorporation of a high content of an alkaline earth oxide (BaO) as in the LBPB3 sample [12, 14, 15, 16].

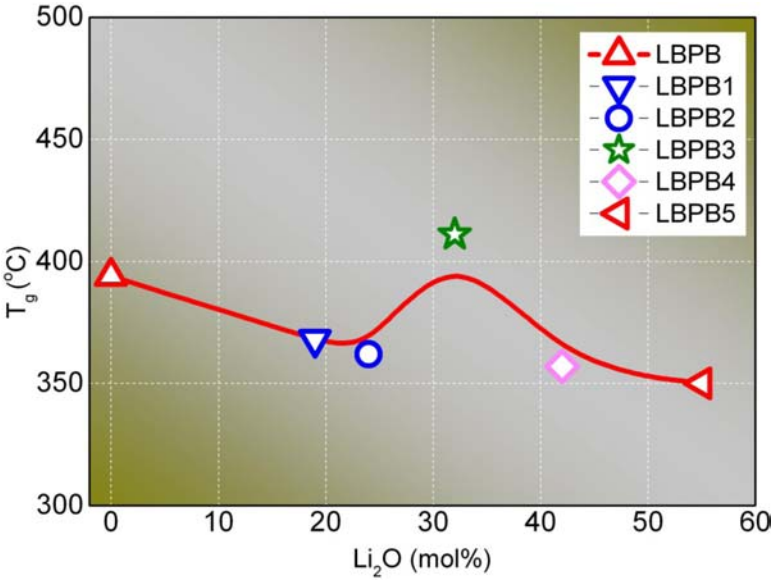

Figure 4. T_g as a function of lithium oxide content.

Some of the most important problems of solid state batteries are the low ionic conductivity of the solid electrolyte and the electrode/electrolyte interfacial compatibility [17] which is a great challenge to overcome. In this work, we manage the ionic conductivity behaviour of an outstanding glassy electrolyte. Astoundingly, we improve its conductivity in five magnitude orders only increasing the lithium ion content without inducing dramatic changes in the glassy matrix. We reach a conductivity value of the order of 10^{-4} S.cm^{-1} at relative low temperature as Figure 5 shows, where the isothermal conductivity at 441K increases almost linearly with the increase in the lithium oxide content. Moreover, our main goal was to obtain an environmental friendly glassy matrix which additionally is a low cost material because of any of its components is toxic and they are abundant enough on the Earth's crust to have a small price at the international market [3]. Moreover, our electrolyte is able to storage a huge quantity of mobile lithium ions.

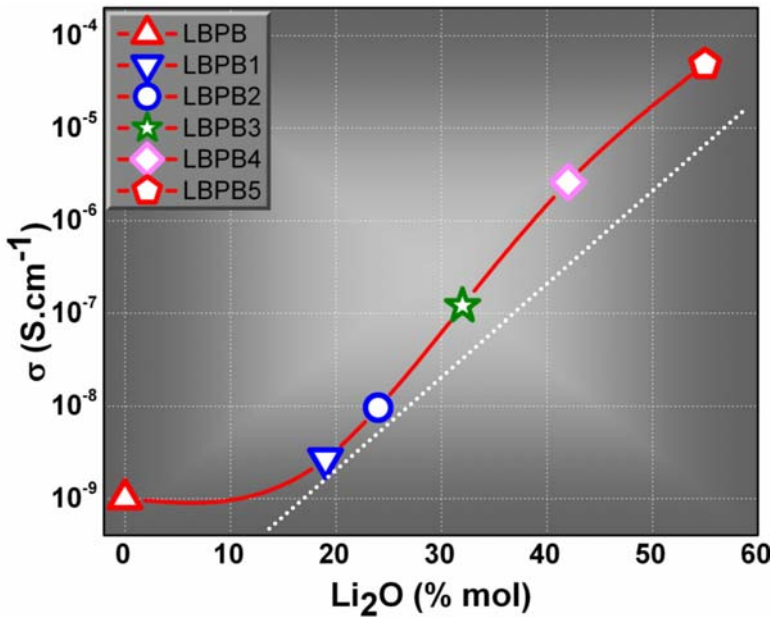

Figure 5. Isothermal electrical dc conductivity (T = 441K) as a function lithium oxide content.

Electrical conductivity relaxation measurements of ionic conducting glasses are commonly analyzed through the real part of the complex conductivity and electric modulus. The ac conductivity spectrum, σ_{ϖ}, of the studied glasses in the present work -over a wide range of temperature and frequency- shows a region of power-law behaviour according to the following expression:

$$\sigma_{(\omega)} = \sigma_{(0)} + A^{s}, \tag{1}$$

where ϖ is the angular frequency, $\sigma_{(0)}$ is the dc conductivity $(\text{at } \varpi \to 0)$ and s is a fractional exponent. Both $\sigma_{(0)}$ and A are thermally activated quantities. Jonscher and Ngai [18, 19, 20] called this behaviour as the 'universal dynamic response' (UDR) because of the wide variety of materials that showed it. Figure 6 shows the conductivity spectra of our best lithium conductor in this work, LBPB5 at low and high temperature bellow its T_g.

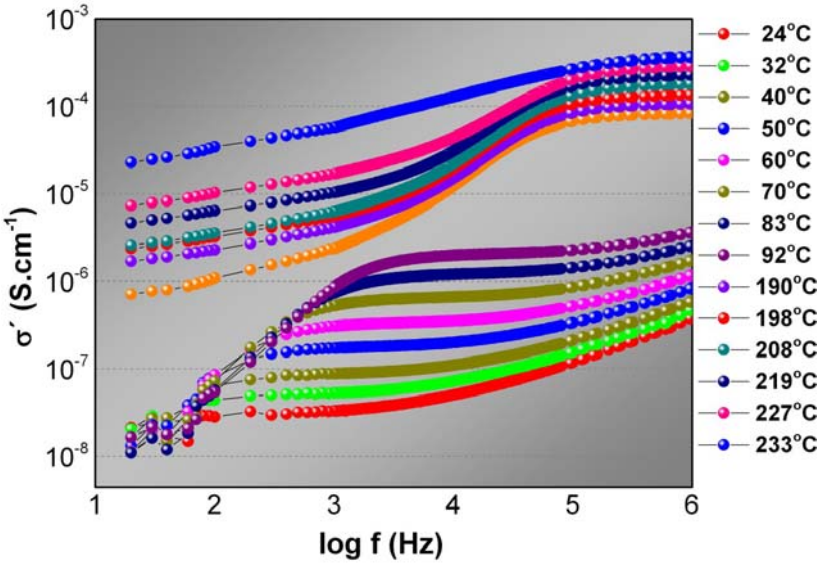

Figure 6. Real part of the complex conductivity as a function of the frequency of LBPB5.

The characterization of the dielectric relaxation in ionic glasses is well described through the modulus representation. The complex modulus applied to materials with non zero dc conductivity is related to the complex conductivity by the expression [21, 22]:

$$\sigma^* = \frac{i\omega\varepsilon_0}{M^*_\omega}, \tag{2}$$

where ε_0 is the vacuum permittivity.

On the other hand, the electric modulus formalism considers the electrical response as a function of frequency similar to shear stress relaxation in liquids where it approaches to a new equilibrium state after being perturbed in terms of a relaxation function in the time domain [20, 23]. The phenomenological nature of the electric modulus [24] is used to make a correlation between the conductivity and the relaxation of mobile ions in these glasses which consider the low-frequency value of M' is zero and represents a lack of restoring force for the electric field induced mobile alkali ions. When the frequency increases M' increasing and reaches a maximum asymptotic value M_∞ at high frequency. The

M'' spectrum exhibits a maximum $M''_{\max}$ centered at the dispersion region of $M'_{(\omega)}$ and its position shifts to higher frequency when the temperature increases. This $M''_{\max}$ determines the range in which charge carriers are mobile over long distances and in the region above the peak maximum the carriers are confined to potential wells being mobile over short distances. The frequency corresponding to the $M''_{\max}$ gives the most probable relaxation time τ for the ions and it follows a temperature Arrhenius behaviour with an activation energy (E_τ) [25]. For charge carriers vibrating in their cages and hopping to neighbouring sites through barriers of energy its relaxation time for independent hopping is:

$$\tau_{o(T)} = \tau_\infty \exp(E_\tau / kT). \tag{3}$$

Figure 7 shows the imaginary part of the complex electric modulus as a function of the frequency for our best studied ionic conductor in the present work, LBPB5. These curves show the relaxation process which shifts towards lower frequencies when the temperature diminishes.

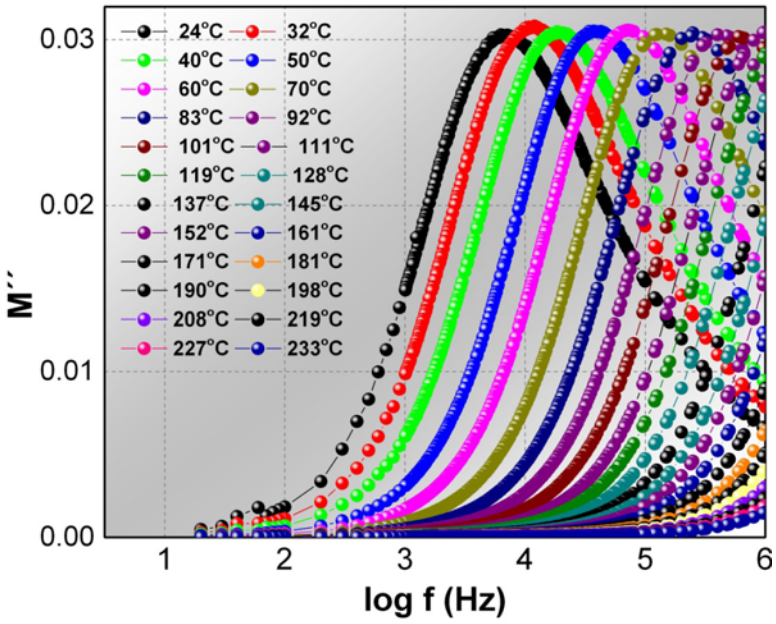

Figure 7. Imaginary part of the complex electric modulus as a function of the frequency of LBPB5.

The peak frequency corresponding to $M''_{\max}$ gives the most probable relaxation time or the mean electric field relaxation time because of the condition $\omega . < \tau >= 1$. Figure 8 shows that both the conductivity and the peak frequency obey the Arrhenius relation according to the expressions (3) and (4), respectively:

$$\sigma_{(dc)} = \sigma_0 \exp(- E_{dc} / kT). \quad (4)$$

From the corresponding slops in Figure 8, the activation energies in the Equations (3) and (4) have been determined and their values are listed on the right in the Figure 8.

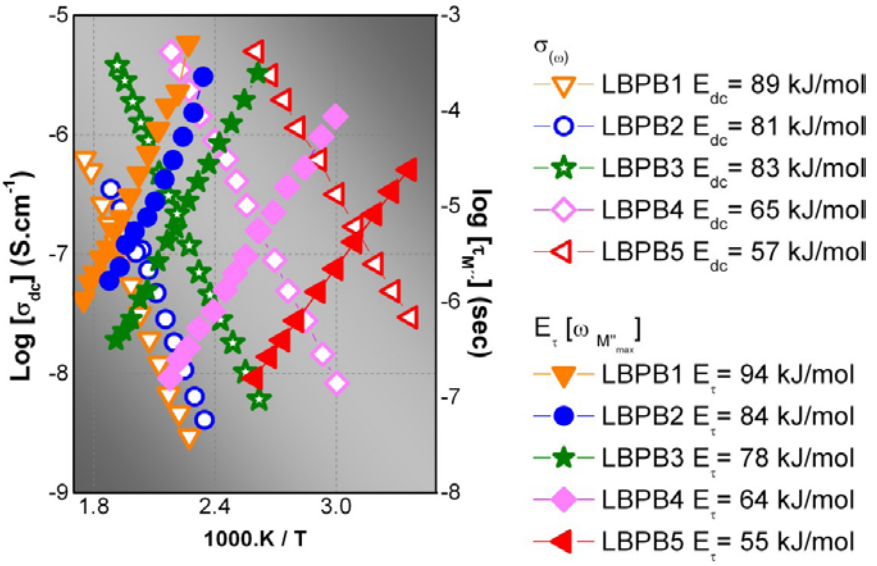

Figure 8. Arrhenius plot of σ_{dc} and τ according to Equations (3) and (4). On the right side, the corresponding activation energies, E_{dc} and E_{τ}, for each sample.

The complex modulus activation energy (E_{τ}) obtained from the slop in Figure 8 is close to the conductivity energy (E_{dc}) in the range of the experimental temperature. From those data, we learn that both activation energies, E_{dc} and E_{τ}, diminish strongly when the content of Li_2O increases and the variation in the BaO content does not show any influence on the energy barrier that the charge carrier, lithium ion, has to overcome.

Additionally, Figure 9 shows a master plot for the imaginary part of the electric modulus ($\log M''_{\omega} / M''_{\omega max}$]) as a function of ($\log f/f_{max}$]) at various temperatures for every sample. The shape of those curves overlaps very well. This result indicates that the dynamic process is temperature independent.

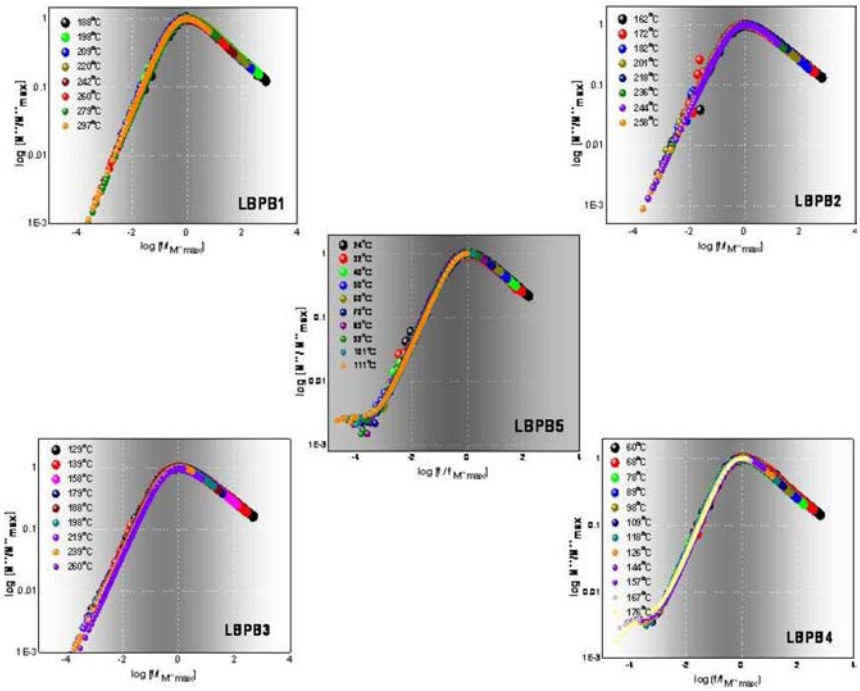

Figure 9. Master plot of the imaginary part of the electric modulus ($\log M''_{\omega} / M''_{\omega max}$]) as a function of ($\log f/f_{max}$]) at various temperatures.

Finally, in Figure 10 we show the FTIR spectra. We have done the spectrum deconvolution and the bands assignment is in Table 1. The strong intensity observed for bands 3 and 4 is assumed that is caused by the high content of lithium cation and that suggests a presence of a high concentration of non-bridging oxygen (NBO) which provides a large number of available sites for the ion hopping and facilitates the mechanism of the charge transport [26, 27, 28].

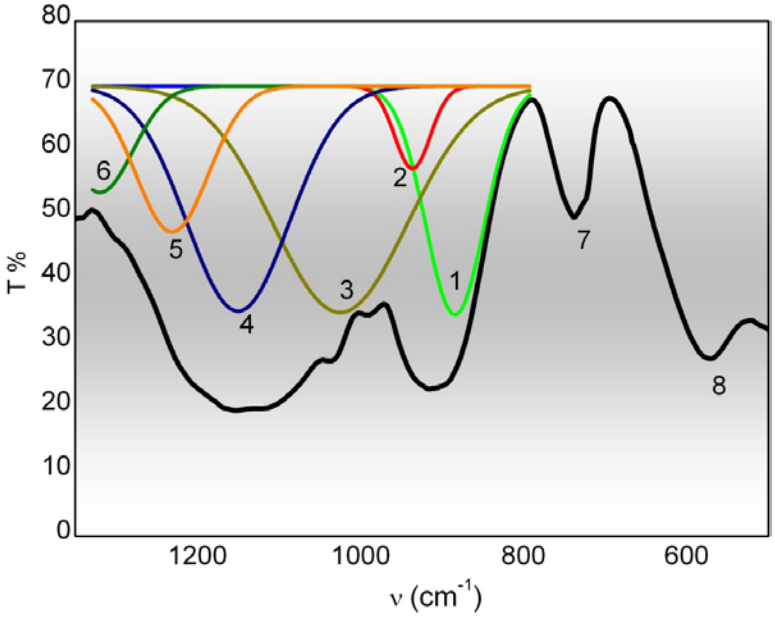

Figure 10. FTIR spectrum at room temperature of LBPB5 sample.

Table 1. Bands assignment belonging to the FTIR spectrum of LBPB5 sample

Bands	
1	$\bar{\nu}_s$ and $\bar{\nu}_{antisym\ stretch}$ (P-O-P groups) in Q^1 and Q^2 structural units
2	
3	PO_4^{3-} groups in Q^0 structural units
4	PO_4^{2-} groups in Q^1 structural units
5	$\bar{\nu}_s$ and $\bar{\nu}_{antisym\ stretch}$ (PO_2) groups in Q^2 structural units
6	
7	P–O–P $\bar{\nu}_{antisym\ stretch}$ in Q^1 structural units
8	$\bar{\nu}_s$ Ba–O–P bonds

Considering that the change of polarization direction in response to the external field is characterized by a time constant of the material, known as relaxation time τ and, when a dielectric dispersion occurs over a broad frequency range it is required the use of a distribution of relaxation times to obtain a good fit of the dielectric data, the polarization itself involves movement of ions which in glasses have to overcome an energy barrier for hopping. Therefore, it is necessary to assume that there is a distribution of barriers which results in a distribution of relaxation times. Since ionic hopping is an activated process and follows a temperature dependence Arrhenius type, the relaxation time characterizes the motion of an ion between equivalent positions around a NBO. However, the diffusion controlled relaxation model is based on the same assumptions as those made in Anderson-Stuart (1954) model to describe non-local and local ionic motions. Elliott (in 1987, 1988, 1989) has approached the relaxation problem in DCR model and he considered the ionic motion by a local motion of cations among equivalent positions located around a NBO ion which causes the primary relaxational event and it occurs with a characteristic microscopic relaxation time *t* and this process gives rise to a polarization current. When another cation hops intoone of the nearby equivalent positions a double occupancy results around the anion and this makes the relaxation instantaneous involving the diffusion of a cation and because of that the whole process involves both polarization and diffusion currents.

The origin of the non-Debye behaviour of relaxations (distribution of relaxation times) has also been discussed in terms of inter-ionic Coulombic interactions: Nowick et al. (1994) have shown that in the region of temperature between constant loss regime and Jonscher's regimes (where *s* parameter in Equation (1) drops from a value of 1.0 to ~ 0.6) it is possible to treat the data as a superposition of both regimes. Such power law is now widely employed in the analysis of conductivity behaviour. The exponent value of 0.6 in Jonscher's regime is considered to arise by the ion-ion interactions, usually of the coulombic type [11].

From the data fitting of our results of $\sigma_{(\omega)}$, we found that *s* takes values between 0.61 and 0.85 for every lithium modified sample studied here. Taking into account the interaction model explained before, during the process of the hopping of the ions -even separate hopping events- may have a broad distribution of relaxation times and this effect can manifest as stretching of the relaxation times. Ngai's coupling model accounts for stretched exponential relaxation and considers it as a consequence of switching on the coulombic interactions. Hence, from the analysis of our results presented in Figures 8 and 9, the ion interactions in the lithium conducting glasses presented in this work act favorably considering the enormous reduction in the activation energy both for conduction as for electric relaxation time. It is possible to suppose the presence of a huge concentration of mobile ions (charge carriers) with a high mobility and as consequence the material conductivity is improved.

4. Conclusion

In this work, we have presented the result of the electrical property of a new and improved phosphate modified glass composition. This material could be used as solid electrolyte to develop all solid state secondary lithium batteries. The incorporation of other oxides as the mix of an appropriated quantity of BaO and Bi_2O_3 has shown a great impact on the glass matrix stability. We have developed a boosted glass composition which allows the incorporation of a huge content of lithium oxide. As a result, a lithium solid electrolyte with high ionic conductivity at moderate temperature has been obtained with low activation energy for the ionic transport without losing the matrix stability. Lithium solid electrolytes, as the material of the present work, are waiting for a detailed explanation the mechanism involved in the charge transport as has been reported in the literature for many polymer systems [29] (and references there in).

Acknowledgements

Financial support by CONICET and Universidad Nacional del Sur is gratefully acknowledged. P. E. dP and S. T. are Fellows of the CONICET. M. E. S. is UNS Researcher and M. A. F. is Researcher Fellow of CONICET – Argentina.

References

[1] J.-M. Tarascon and M. Armand, Nature 414 (2001), 359-367.

[2] C. Liu, F. Li, L.-P. Ma and H.-M. Cheng, Advanced Materials for Energy Storage 22 (2010), E28-E62.

[3] N. Nitta, F. Wu, J. T. Lee and G. Yushin, Materials Today 18(5) (2015), 252-264.

[4] P. G. Balakrishnan, R. Ramesh and T. Prem Kumar, Journal of Power Sources 155 (2006), 401-414.

[5] L. Oliveira, M. Messagie, S. Rangaraju, J. Sanfelix, M. Hernandez Rivas and J. Van Mierlo, Journal of Cleaner Production 108 (2015), 354-362.

[6] S. Hazra, S. Mandal and A. Ghosh, Physical Review B 56(13) (1997), 8021-8025.

[7] D. W. Hall, M. A. Newhouse, N. F. Borrelli, W. H. Dumbaugh and D. L. Weidman, Appl. Phys. Lett. 54 (1989), 1293-1295.

[8] W. H. Dumbaugh, Phys. Chem. Glasses 19(6) (1978), 121-125.

[9] D. L. Sidebottom, Physical Review B 61(21) (2000), 14507-14516.

[10] J. Fu, Phys. Chem. Glasses 37 (1996), 84-92.

[11] K. J. Rao, Structural Chemistry of Glasses, Chapter 7, First Ed. 2002. ISBN 0-08-043958-6. Elsevier (and reference there in).

[12] P. E. di Prátula, S. Terny, E. C. Cardillo and M. A. Frechero, Solid State Sciences 49 (2015), 83-89.

[13] C. S. Terny, E. C. Cardillo, P. E. di Prátula, M. A. Villar and M. A. Frechero, Journal of Non-Crystalline Solids 387 (2014), 107-111.

[14] S. Terny, M. A. De la Rubia, R. E. Alonso, J. de Frutos and M. A. Frechero, Journal of Non-Crystalline Solids 411 (2015), 13-18.

[15] S. Terny, M. De La Rubia, S. Barolin, R. E. Alonso, J. De Frutos and M. A. Frechero, Boletin de la Sociedad Española de Ceramica y Vidrio 53 (1) (2014), 15-20.

[16] S. Terny, M. A. De la Rubia, J. De Frutos and M. A. Frechero, Journal of Non-Crystalline Solids 433 (2016), 68-74.

[17] J. Li, C. Ma, M. Chi, C. Liang and N. J. Dudney, Adv. Energy Mater. (2014), 1401408.

[18] A. K. Jonscher, Nature 267 (1977), 673.

[19] K. L. Ngai, Comments Solid State Phys. 9 (1979), 127.

[20] K. L. Ngai, Comments Solid State Phys. 9 (1980), 141.

[21] 3- P. Macedo, C. Moynihan and R. Bose, Phys. Chem. Glasses 13 (1972), 171-179.

[22] A. S. Nowick, A. V. Vaysleyb and Wu Liu, Solid State Ionics 105 (1998), 121-128.

[23] V. Provenzano, L. P. Boesch, V. Volterra, C. T. Moynihan and P. B. Macedo, J. Am. Ceram. Soc. 55 (1972), 492-496.

[24] K. L. Ngai and S. W. Martin, Phys. Rev. B 40 (1989), 10550-10556.

[25] A. Dutta, T. P. Sinha, P. Jena and S. Adak, Journal of Non-Crystalline Solids 354 (2008), 3952-3957.

[26] P. Srinivasa Rao, Ch. Rajyasree, A. Ramesh Babu, P. M. Vinaya Teja and D. Krishna Rao, Journal of Non-Crystalline Solids 357 (2011), 3585-3591.

[27] M. Lu, F. Wang, K. Chen, Y. Dai, Q. Liao and H. Zhu, Spectrochimica Acta Part A: Molecular and Biomolecular Spectroscopy 148 (2015), 1-6.

[28] P. K. Jha, O. P. Pandey and K. Singh, Journal of Molecular Structure 1094 (2015), 174-182.

[29] S. Xue, Y. Liu, H. Dang, Y. Li, D. Teeters, D. W. Crunkleton and S. Wang, Computational Materials Science 12 (2016), 170-174.

■